J. Biochem. **133**, 75–81 (2003)
DOI: 10.1093/jb/mvg011

Crystal Structure of Hyperthermophilic Archaeal Initiation Factor 5A: A Homologue of Eukaryotic Initiation Factor 5A (eIF-5A)

Min Yao[1], Akiko Ohsawa[2], Shingo Kikukawa[2], Isao Tanaka[1] and Makoto Kimura[*,2]

[1]*Division of Biological Science, Graduate School of Science, Hokkaido University, Sapporo 066-0810; and*
[2]*Laboratory of Biochemistry, Department of Bioscience and Biotechnology, Faculty of Agriculture, Graduate School, Kyushu University, Fukuoka 812-8581*

Received October 4, 2002; accepted October 25, 2002

Eukaryotic initiation factor 5A (eIF-5A) is ubiquitous in eukaryotes and archaebacteria and is essential for cell proliferation and survival. The crystal structure of the eIF-5A homologue (*Pho*IF-5A) from a hyperthermophilic archaebacterium *Pyrococcus horikoshii* OT3 was determined at 2.0 Å resolution by the molecular replacement method. *Pho*IF-5A is predominantly composed of β-strands comprising two distinct folding domains, an N-domain (residues 1–69) and a C-domain (residues 72–138), connected by a short linker peptide (residues 70–71). The N-domain has an SH3-like barrel, while the C-domain folds in an (oligonucleotide/oligosaccharide binding) OB fold. Comparison of the structure of *Pho*IF-5A with those of archaeal homologues from *Methanococcus jannaschii* and *Pyrobaculum aerophilum* showed that the N-domains could be superimposed with root mean square deviation (rmsd) values of 0.679 and 0.624 Å, while the C-domains gave higher values of 1.824 and 1.329 Å, respectively. Several lines of evidence suggest that eIF-5A functions as a biomodular protein capable of interacting with protein and nucleic acid. The surface representation of electrostatic potential shows that *Pho*IF-5A has a concave surface with positively charged residues between the N- and C-domains. In addition, a flexible long hairpin loop, L1 (residues 33–41), with a hypusine modification site is positively charged, protruding from the N-domain. In contrast, the opposite side of the concave surface at the C-domain is mostly negatively charged. These findings led to the speculation that the concave surface and loop L1 at the N-domain may be involved in RNA binding, while the opposite side of the concave surface in the C-domain may be involved in protein interaction.

Key words: archaebacteria, crystal structure, initiation factor 5A, *Pyrococcus horikoshii*.

Abbreviations: eIF-5A, eukaryotic initiation factor 5A; *Mja*IF-5A, initiation factor 5A from *Methanococcus jannaschii*; NCS, non-crystallographic symmetry; OB-fold, oligonucleotide/oligosaccharide binding fold; *Pae*IF-5A, initiation factor 5A from *Pyrobaculum aerophilum*; PEG, polyethylene glycol; *Pho*IF-5A, initiation factor 5A from *Pyrococcus horikoshii*; rmsd, root mean square deviation.

Eukaryotic initiation factor 5A (eIF-5A), ubiquitous in both eukaryotes and archaebacteria, consists of about 140 amino acid residues and was initially named based on the findings that eIF-5A could be isolated from the ribosome-bound fraction and stimulate the synthesis of methionyl-puromycin (*1*, *2*). However, the role of eIF-5A in translation initiation has been questioned because of a lack of correlation between eIF-5A and general protein synthesis (*3*). Alternatively, it was proposed that eIF-5A may facilitate protein synthesis by promoting nuclear export of specific mRNAs (*4*). Furthermore, a recent study has suggested that eIF-5A may facilitate the translation of mRNA species required for programmed cell death (*5*).

eIF-5A is the only cellular protein known to contain a hypusine residue (for review, see Refs. *6* and *7*). Hypusine is formed by a series of post-translational reactions. The first reaction leading to the formation of hypusine is catalyzed by deoxyhypusine synthase, an enzyme that adds butylamine to the conserved lysine of eIF-5A to form deoxyhypusine. A subsequent reaction in which deoxyhypusine is converted to hypusine is catalyzed by deoxyhypusine hydroxylase (*8–10*). Hypusine formation is tightly coupled to cell proliferation and is essential for cell survival (*11*, *12*). Disruption of either eIF-5A or the deoxyhypusine synthesis gene in yeast leads to a lethal phenotype (*13*, *14*). Recently, it was reported that hypusine is required for a sequence-specific interaction of eIF-5A with RNA (*15*).

Although eIF-5A is essential for cell proliferation and survival, the precise physiological function of eIF-5A is still unclear. In this study, we determined the crystal structure of an eIF-5A homologue (*Pho*IF-5A) from the hyperthermophilic archaebacterium *Pyrococcus horikoshii* OT3 in the hopes that it would be of help in understanding the cellular function and role of eIF-5A. *P.*

[*]To whom correspondence should be addressed. Tel/Fax: +81-92-642-2853, E-mail: mkimura@agr.kyushu-u.ac.jp

Table 1. **Summary of data collection.**

Space group	$P3_2$
Unit cell	$a = b = 93.3$ Å, $c = 39.2$ Å, $\gamma = 120°$
Z'[a]	3 ($V_M = 2.16$ Å^3/Da)
Wavelength (Å)	0.90
Resolution (Å)[b]	100–2.0 (2.11–2.0)
Number of observed reflections	148,604
Unique reflections	25,949
Completeness (%)	100 (99.9)
Averaged redundancy	5.7 (5.7)
Averaged $I/\sigma(I)$	8.5 (2.4)
R_{means} (%)[c]	8.1 (34.9)

[a]Z' is the number of molecules in an asymmetric unit. [b]Values in parentheses are for the outermost resolution shell. [c]$R_{means} = \Sigma_h[m/(m-1)]^{1/2}\Sigma_j|\langle I\rangle_h - I_{h,j}|\Sigma_h\Sigma_j I_{h,j}$, where $\langle I\rangle_h$ is the mean intensity of symmetry-equivalent reflections and m is redundancy.

horikoshii OT3 isolated from the hot waters of the Okinawa Trench can grow at high temperatures, favoring a temperature of 98°C. The entire length of the genome is 1.74 million base pairs, comprising 2,061 open reading frames. The functions of about 27% of the *P. horikoshii* gene products can be assigned based on their amino acid sequence analysis (*16*). A gene (ID code PH1381) product was assigned as the homologue of eIF-5A, sharing 22% identical residues with *Saccharomyces cerevisiae* eIF-5A. Here, we report the three-dimensional structure of *Pho*IF-5A determined at 2.0 Å resolution by the molecular replacement method using eIF-5A homologues from *Methanococcus jannaschii* (PDB code 2EIF) (*17*) and *Pyrobaculum aerophilum* (PDB code 1BKB) (*18*) as search models.

MATERIALS AND METHODS

Materials—Restriction enzymes were purchased from MBI Fermentas. The oligonucleotide primers and thermo sequenase fluorescent labeled primer cycle sequencing kit containing 7-deaza-dGTP were obtained from Amersham Pharmacia Biotech. Plasmid pGEM T-vector and expression plasmid pET-22b were obtained from Promega and Novagen, respectively. *Escherichia coli* strains JM109 and BL21 (DE3) were used as host cells for cloning and producing recombinant protein, respectively. Polyethylene glycol 4000 (PEG 4000) was obtained from Fluka Chemicals; reagents were purchased at the highest purity available.

Cloning, Overproduction, and Purification—The gene (ID code PH1381) encoding the *P. horikoshii* IF-5A (*Pho*IF-5A) was amplified by PCR and placed under control of the T7 phage promoter on the expression plasmid pET-22b (*19*). Expression was induced with IPTG, and the resulting protein was purified to apparent homogeneity by ion-exchange chromatography on S-Sepharose.

Crystallization and Data Collection—The purified protein *Pho*IF-5A was concentrated to 10 mg ml^{-1} in 0.1 M Hepes-NaOH buffer (pH 7.5). Crystallization attempts were made by the hanging-drop vapor diffusion method at 18°C using crystal screen kits (Hampton Research) as reservoir solutions. Each drop was formed by mixing equal volumes (2 µl:2 µl) of protein and reservoir solution. Crystals of *Pho*IF-5A were obtained under conditions of 10% isopropanol and 20% PEG 4000 in one week with a size of $0.1 \times 0.1 \times 0.2$ mm^3.

For data collection, the crystals of *Pho*IF-5A were transferred into a cryoprotectant solution containing 20% sucrose in reservoir solution, then mounted in a nylon loop and flash-frozen in a nitrogen stream at 100 K. X-ray diffraction data were collected on beamline BL41XU at SPring-8 of Japan, integrated, scaled and merged by the MOSFLM (*20*) and SCALA (*21*) programs. A crystal of *Pho*IF-5A diffracts to 2.0 Å and belongs to space group $P3_2$ with cell dimensions of $a = b = 93.3$ Å, $c = 39.4$ Å, and $\gamma = 120°$. Crystals of *Pho*IF-5A contain three molecules per asymmetric unit, corresponding to a V_M of 2.16 Å^3 Da^{-1}. Assuming a value of 0.74 cm^3 g^{-1} for the protein partial specific volume (*22*), the calculated solvent content in the crystal is 43.1%. The statistics of data collection are summarized in Table 1.

Structure Determination and Refinement—The crystal structure of *Pho*IF-5A was determined by the molecular replacement method using the program MOLREP (*23*). Two search models of archaeal homologues from *M. jannaschii* (ID: 2EIF) and *P. aerophilum* (ID: 1BKB), which have 46.4 and 48% identical residues with *Pho*IF-5A, respectively, were constructed based on the alignment of amino acid sequences. Structure refinement was performed using the program CNS (*24*), and the 10% reflection data were set aside for the calculation of the free *R*-factor to monitor the refinement. After the first step of the refinement at 2.5 Å resolution, a model of *Pho*IF5A was rebuilt using the program O (*25*). Non-crystallographic symmetry (NCS) restraints were applied throughout the refinement. The coordinates have been deposited in the Protein Data Bank (ID: 1IZ6).

RESULTS AND DISCUSSION

Structure Determination and Quality—In spite of the presence of three independent molecules (MolA, MolB, and MolC) in an asymmetry unit, the self-rotation function did not reveal any local symmetry. However, the native Patterson function that was subsequently calculated showed a peak at translation vector [0.67, 0.33, 0.43] (fractional coordinate), which means that at least two molecules have nearly identical orientations in the asymmetric unit. Table 2 shows the results of the molecular replacement calculated by the program MOLREP. The best solution was obtained from space group $P3_2$ and a search model of 1BKB, which gave a correlation coefficient of 40.3% and an *R* factor of 52.5%. Two of the three independent molecules have nearly identical orientations with a shift vector of [0.67, 0.33, 0.43].

The initial model constructed from 1BKB contained 134 residues (out of a total 136 residues) of which 62 residues possessed full side chains. After generating all side chains by computer, the first round of refinement, including rigid-body, positional, temperature and simulated annealing, was carried out at 2.5 Å resolution, which gave free *R*- and *R*-factors of 42.9 and 33.4%, respectively. The structure was remodeled using program O. After several rounds of refinement and manual fitting, the structure was refined to the free *R*- and *R*-factors of 23.7 and 19.9%, respectively, at 2.0 Å resolu-

Table 2. **Cross-rotation and translation function statistics.**

Model		θ1 (°)	θ2 (°)	θ3(°)	*x*	*y*	*z*	CC (%)	*R* (%)
	Cross rotation function ($P3_x$)								
1BKB	answer1	22.79	67.92	–81.54				4.56	
	answer2	87.68	57.23	74.66				4.36	
	answer3	44.06	104.45	37.07				4.02	
	answer4	39.06	37.91	–80.41				3.73	
	answer5	57.39	69.98	183.05				3.72	
2EIF	answer1	58.87	107.00	32.9				4.38	
	answer2	82.72	100.71	66.89				4.09	
	answer3	75.60	72.56	119.94				4.08	
	answer4	65.06	108.67	45.80				3.88	
	answer5	4.33	46.90	127.29				3.80	
	Translation function								
1BKB	$P3_2$								
	Third site using two sites of (22.79, 67.92, –81.54, 0.167, 0.118, 0.000) and (32.69, 38.81, –75.54, 0.797, 0.448, 0.334)								
	answer1	39.06	37.91	–80.41	0.462	0.789	0.771	40.5	52.5
	answer2	39.06	37.91	–80.41	0.381	0.777	0.044	36.3	54.4
	answer3	39.06	37.91	–80.41	0.477	0.688	0.815	36.1	54.0
	$P3_1$								
	Third site using two sites of (22.79, 67.92, –81.50, 0.607, 0.288, 0.000) and (39.06, 37.91, –80.41, 0.189, 0.239, 0.695)								
	answer1	22.79	67.92	–81.54	0.277	0.624	0.431	31.4	56.9
	answer2	22.79	67.92	–81.54	0.218	0.144	0.036	30.3	56.7
	answer3	22.79	67.92	–81.54	0.099	0.788	0.944	30.3	56.8
2EIF	$P3_2$								
	Third site using two sites of (58.87, 107.00, 32.95, 0.878, 0.050, 0.000) and (82.72, 100.71, 66.89, 0.544, 0.345, 0.332)								
	answer1	82.72	100.71	66.89	0.203	0.674	0.758	36.9	54.6
	answer2	82.72	100.71	66.89	0.207	0.672	0.649	32.7	55.8
	answer3	82.72	100.71	66.89	0.194	0.643	0.874	32.6	55.6
	$P3_1$								
	Third site using two sites of (58.87, 107.00, 32.95, 0.377, 0.284, 0.000) and (82.72, 100.71, 66.89, 0.056, 0.362, 0.584)								
	answer1	32.38	50.18	–65.46	0.394	0.421	0.082	31.5	55.8
	answer2	32.38	50.18	–65.46	0.713	0.471	0.874	30.7	56.2
	answer3	32.38	50.18	–65.46	0.200	0.295	0.534	30.7	56.3

Table 3. **Final refinement statistics.**

Resolution range (Å)	10.0–2.0
Number of reflections	25,746
Completeness (%)	100
Total number of non-hydrogen atoms	
Protein	3,158
Solvent	279
R-factor (%)[a]	18.5
R-free-factor (%)[b]	23.6
rmsd deviation from standard values	
Bond lengths (Å)	0.009
Bond angles (deg)	1.628
Average *B*-factor (Å^2)	
Protein	27.7
Solvent	37.4
Ramachandran plot[c]	
Residues in most favored regions (%)	91.2
Residues in additional allowed regions (%)	8.8

[a]*R*-factor = $\Sigma | F_{obs} - F_{cal} | / \Sigma F_{obs}$, where F_{obs} and F_{cal} are observed and calculated structure factor amplitudes. [b]*R*-free-factor value was calculated for *R*-factor, using only an unrefined subset of reflections data (10%). [c]Ramachandran plot was calculated by PROCHECK (*26*).

tion. The refined structure contains 407 residues [136 (MolA), 136 (MolB), and 135 (MolC)] and 278 water molecules in the asymmetric unit. The N-terminal Met and C-terminal Gln residues are disordered, and the loop L1 (residues 33–41) has weak density. The model has geometries close to ideal with rmsd of 0.009 Å and 1.5° from ideal values for bond lengths and angles, respectively. When the structure was checked using PROCHECK (*26*), 91.2% of the non-glycine and non-proline residues fell in the most favored regions and 8.8% in the additional allowed region of the Ramachandran plot. The refinement statistics are summarized in Table 3.

Overall Structure—The refined model of *Pho*IF-5A is a beta-rich structure with 52.9% β-strand, 8.0% helical (including 3_{10}-helix), 18% turn, and 27.1% unclassified coil. *Pho*IF-5A consists of two distinct domains, an N-domain (residues 1–69) and a C-domain (residues 72–138) (Fig. 1). The secondary structure of *Pho*IF-5A as defined by the program DSSP (*27*) is shown in Fig. 2. The N-domain has an SH3-like barrel motif consisting of a 3_{10}-helix (α1) and six-stranded (β1, β2, β3, β4, β5, and β6) anti-parallel highly twisted β-sheets. The N-domain has a long hairpin loop, L1 (residues 33–41), including a specific residue, Lys37, that is supposed to be modified to hypusine residue. A quarter of the long β3 strand forms hydrogen bonds with β2, and the remaining part with β4. The β2 strand and the N-terminal portion of β3 are approximately perpendicular to strands β3, β4, β5, and β6. This highly twisted β-sheet forms a distorted β-barrel with a short 3_{10}-helix on the top. Further, hydrophobic residues Val7, Val9, Leu12, Ile18, Ile20, Ile27, Val32, Ala43, Ile45, Ile58, Val66, and Val68 form a hydrophobic core inside the β-barrel.

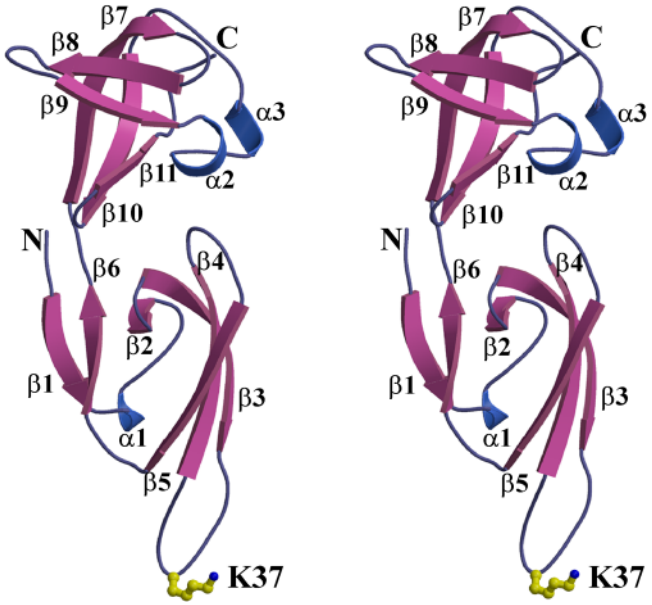

Fig. 1. **A stereoscopic drawing of the translation initiation factor *Pho*IF-5A from *P. horikoshii*.** The balls-and-sticks represent the specific amino acid Lys37 that is supposed to be modified to hypusine.

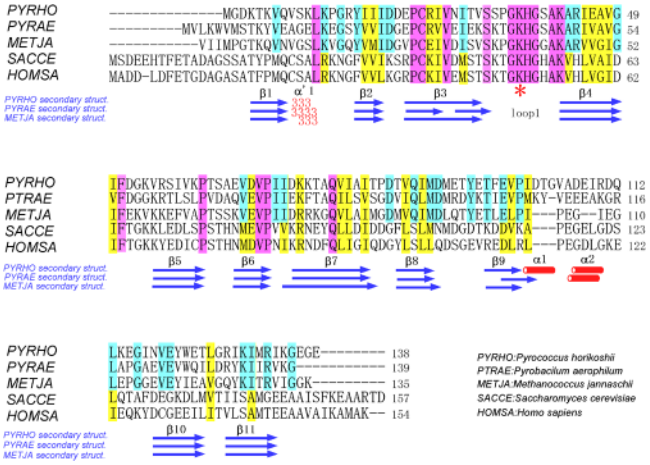

Fig. 2. **Sequence comparison of the translation initiation factor 5As.** The alignment of amino acid sequences was first calculated by CLUSTAL W (*28*) and modified based on the secondary structures of *Pho*IF-5A (present work), *Mja*IF-5A (*17*), and *Pae*IF-5A (*18*). The amino acid residues are shown as follows: completely identical (pink), conserved change (yellow), completely identical only in archaeal IF-5As (light blue). The secondary structure elements are defined by the DSSP program (*27*). Lys37, which is modified to hypusine, is marked by an asterisk.

The C-domain has an oligonucleotide/oligosaccharide binding fold (OB-fold), comprising two short α-helices (α2 and α3) and a five-stranded (β7, β8, β9, β10, and β11) anti-parallel β-barrel arranged differently from the N-terminal β-barrel. The top of C-terminal β-barrel is capped by a loop between α3 and β10. The long β7 strand forms hydrogen bonds with β8 at the center of the peptide chain. Like the N-domain, the C-terminal β-barrel also forms a hydrophobic core with residues Ala76, Val78, Ile81, Val86, Ile88, Phe97, Val99, Ile101, Val105, Leu113, Val119, and Ile130.

The two domains of *Pho*IF-5A are connected by a peptide linker (residues 70–71), which joins the last β-strand, β6, of N-domain and the first β-strand, β7, of the C-domain. The interface of the two domains is formed by residues from β2, the loop between β4 and β5, and β10. The contact between the two domains involves several hydrogen bonds and a hydrophobic core including residues Tyr17, Pro24, Ile50, Phe51, Ile71, Trp122, Thr124, and Leu125. *Pho*IF-5A has a concave surface between the N- and C-domains with an approximate size of 6.5 Å × 6 Å × 15 Å calculated from the three independent molecules (MolA, MolB, and MolC) in the asymmetry unit.

Structure Comparison—The amino acid sequence of *Pho*IF-5A was aligned with those of two archaeal homologues as well as eukaryotic homologues using the program CLUSTAL W (*28*), as shown in Fig. 2. Most of the conserved sequences are within the N-domain, while the C-domain is less conserved. The overall structure of *Pho*IF-5A displays significant similarity to those of archaeal homologues (Fig. 3a). Superposition of the entire *Pho*IF-5A with the two homologues *Pae*IF-5A and *Mja*IF-5A using the program LSQABK (*29*) gave rmsd values of 1.276 and 1.690 Å, respectively, for 117 Cα atoms. When independent domains were superimposed, the N-domains of the three archaeal IF-5As have a very fixed structure (except loop L1) as shown by the small rmsd values (0.624 and 0.679 Å), whereas the rmsd values of the C-domains are 1.329 and 1.824 Å (Table 4). Distinct rmsd values for the two domains were also obtained by comparison of the three independent molecules of *Pho*IF-5A in the asymmetric unit, as shown in Fig.

Table 4. **Superposition of IF-5As against *Pho*IF-5A (MolA).**

	rmsd[a]				
	Fitting by N-domain[b]		Fitting by C-domain[c]		Fitting by all[d]
	N-domain	C-domain	N-domain	C-domain	
*Pho*IF-5A (MolB)	0.447	2.754	3.861	0.989	1.216
*Pho*IF-5A (MolC)	0.566	2.424	2.977	0.968	1.088
*Pae*IF-5A	0.624	2.325	3.740	1.329	1.276
*Mja*IF-5A	0.679	3.845	4.049	1.824	1.690

[a]rmsd = $(\Sigma_i(\boldsymbol{x}_{i,\text{molecule1}} - \boldsymbol{x}_{i,\text{molecule2}})^2/N)^{1/2}$, $\boldsymbol{x}_i = (x_i, y_i, z_i)$. [b]rmsd values are calculated using Cα atoms of 59 residues (without loop1) and 58 residues in N- and C-domain, respectively, after fitting by N-domain. [c]rmsd values are calculated using Cα atoms of 59 residues (without loop1) and 58 residues in N- and C-domain, respectively, after fitting by C-domain. [d]rmsd values are calculated using Cα atoms of 117 residues.

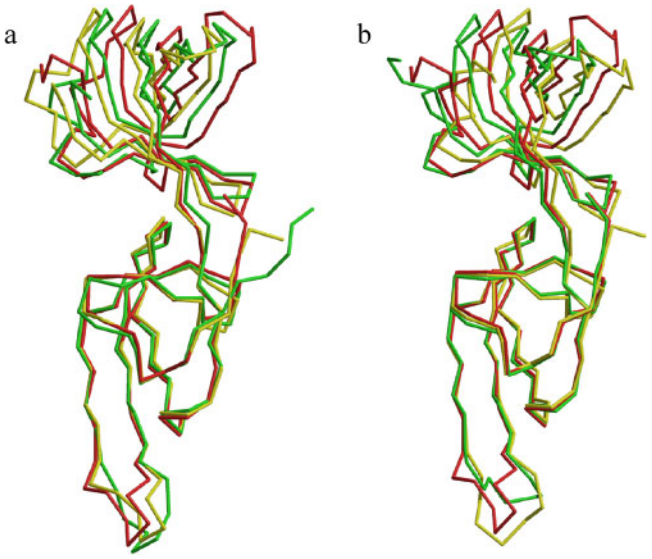

Fig. 3. **Structural comparison of the archaeal IF-5As.** a: Superimposition of the backbone atoms of three archaeal homologues, *Pho*IF-5A (MolA, red), *Pae*IF-5A (green) (*18*), and *Mja*IF-5A (yellow) (*17*). b: Superimposition of the backbone atoms of three independent copies in the asymmetric unit of *Pho*IF-5A; MolA (red), MolB (green), and MolC (yellow).

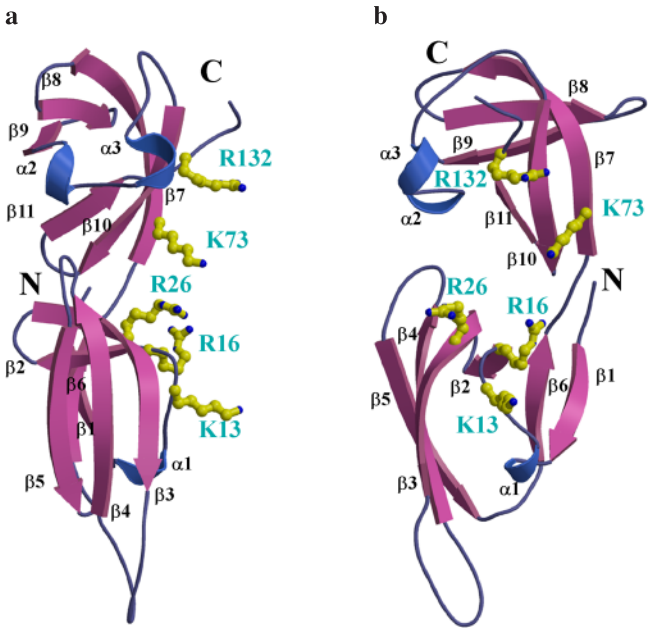

Fig. 5. **A cluster of positively charged residues at the putative RNA-binding region of *Pho*IF-5A.** a: The balls-and-sticks represent positive charged residues that may contribute to RNA binding. b: View rotated 90° from (a).

3b and Table 4, suggesting inter-domain movement within the molecule. Thus, the peptide linker of the two domains mediates an inter-domain flexibility of about 7°.

Possible RNA-Binding Site—The N-domain of *Pho*IF-5A contains an SH3-like barrel motif, while the C-domain folds in an OB-fold. The DALI-server (*30*) shows that SH3-like barrel motifs are found in the DNA binding domain of HIV-integrase (*31*), the repressor of the *E. coli* biotin biosynthetic operon (*32*), and the C-terminal domain of the ribosomal protein L2-RBD (*33*). On the other hand, the OB-fold is one of the most common RNA binding modules and is found in several RNA binding proteins that are known to be associated with translation, including initiation factors, such as IF-1 (*34*) and eIF-2α (*35*), ribosomal proteins, such as S1 (*36*), S17 (*37*), and L2 (*33*), and the N-terminal domain of aspartyl tRNA synthetase (*38*). Interestingly, the ribosomal protein L2-RBD, like eIF-5A, has an SH3-like barrel motif and an OB-fold joined by a flexible peptide (*33*). However, the N-terminal domain of L2-RBD is an OB-fold and the C-terminal domain is an SH3-like barrel, the reverse of the situation in eIF-5A. Nevertheless, these findings strongly suggest that eIF-5A may interact with nucleic

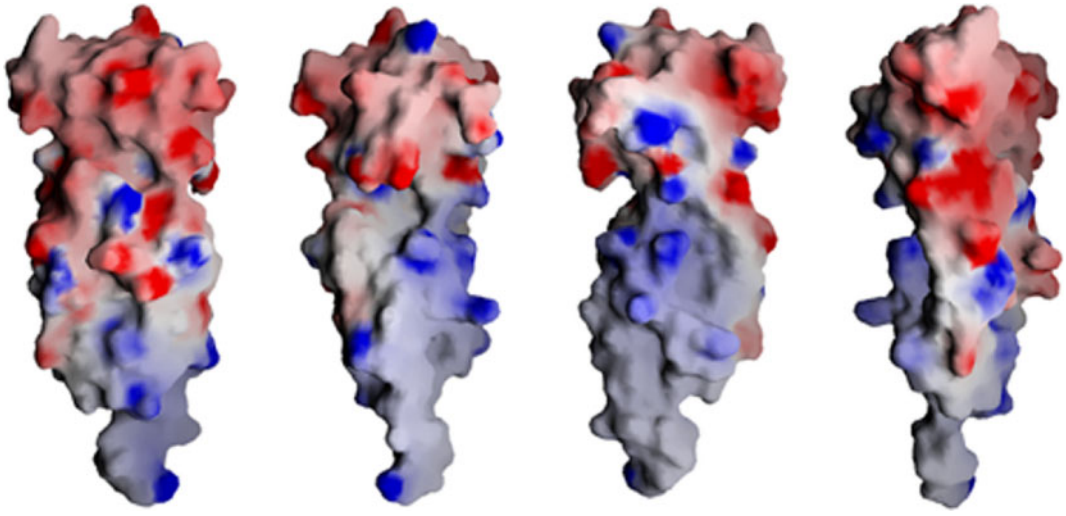

Fig. 4. **Surface representation of the electrostatic potential of *Pho*IF-5A.** Surface representation of the electrostatic potential of *Pho*IF-5A was calculated by GRASP (*46*). The surface potential is displayed as a color gradient from red (negative) to blue (positive). Each view is rotated by 90°.

acids, particularly RNA. Indeed, it is known that eIF-5A is capable of binding to the Rev response element and U6 RNA *in vitro* (*39*). Furthermore, Xu and Chan reported that yeast eIF-5A specifically binds RNA containing the consensus sequence AAAUGUCACAC (*15*). It is generally known that the electrostatic interactions between exposed positively charged residues and the phosphate backbone of RNA, and stacking interactions between exposed aromatic side chains and non-base-paired RNA nucleotides are common features of protein-RNA interactions (*40*). As for the electrostatic potential of *Pho*IF-5A, the concave surface between the N- and C-domains is positively charged, as depicted in Fig. 4. Positively charged residues Lys13, Arg16, and Arg26 in the N-domain, and Lys73 and Arg132 in the C-domain are clustered at the interface of the two domains (Fig. 5). Among them, Lys13 and Lys73 are highly conserved as positive charged residues (either lysine or arginine) in five eIF-5As including yeast and human eIF-5A. In addition, two highly conserved aromatic residues, Tyr17 and Phe51, are located at the valley between the N- and C-domains. These structural features, including inter-domain flexibility, suggest that the concave surface between the N- and C-domains may present a potential surface for interaction with RNA, and that the inter-domain flexibility may become ordered upon RNA binding.

It has been reported that hypusine formation is tightly coupled to cell proliferation and is essential for cell survival (*6*, *7*, *11*). Disruption of either the eIF-5A or deoxyhypusine synthase gene in yeast leads to a lethal phenotype (*12–14*). Further, it has been reported that this modification is required for the RNA binding activity of eIF-5A (*15*). Apparently, a tip of the loop L1 is positively charged, due to the Lys37 and His38 residues. Modification of Lys37 to hypusin further increases the positive charge. It is thus assumed that the tip of loop L1 may be another RNA binding site in eIF-5A, although the possibility that the modification of Lys37 could cause a structural change that results in the formation of an RNA binding site(s) in eIF-5A cannot be excluded. The unambiguous assignment of the RNA binding site must await the determination of the crystal structure of eIF-5A in complex with RNA containing the consensus sequence (*15*).

In contrast, the molecular surface of the opposite side of the concave surface in the C-domain is highly negatively charged, as indicated in Fig. 4. It is thus unlikely that the opposite side of the concave surface of the C-domain interacts directly with RNA. It has been proposed that eIF-5A functions as a bimodular protein, capable of interacting with both protein and nucleic acid (*39*). Indeed, it has been reported that eIF-5A interacts with several proteins, including deoxyhypusine synthase (*41*), transglutaminase II (*42*), L5 (*43*), CRM1 (*44*), and exportin 4 (*45*). It is thus tempting to speculate that eIF-5A may function as a bimodular protein, with RNA binding sites at the concave surface and loop L1, and protein binding sites at the C-domain.

This work was supported in part by a Grant-in-Aid for Scientific Research from the Ministry of Education, Science, Sports and Culture of Japan, and by a grant from the National Project on Protein Structural and Functional Analyses. We thank Dr. M. Kawamoto of the SPring-8, Japan, for his help in data collection and Dr. Y. Kakuta for valuable comments and suggestions on the manuscript.

REFERENCES

1. Kemper, W.M., Berry, K.W., and Merrick, W.C. (1976) Purification and properties of rabbit reticulocyte protein synthesis initiation factors M2Balpha and M2Bbeta. *J. Biol. Chem.* **251**, 5551–5557
2. Benne, R. and Hershey, J.W. (1978) The mechanism of action of protein synthesis initiation factors from rabbit reticulocytes. *J. Biol. Chem.* **253**, 3078–3087
3. Kang, H.A. and Hershey, J.W.B. (1994) Effect of initiation factor eIF-5A depletion on protein synthesis and proliferation of *Saccharomyces cerevisiae*. *J. Biol. Chem.* **269**, 3934–3940
4. Bevec, D. and Hauber, J. (1997) Eukaryotic initiation factor 5A activity and HIV-Rev function. *Biol. Signals* **6**, 124–133
5. Wang, T.-W., Ku, L., Wang, D., and Thompson, J.E. (2001) Isolation and characterization of senescence-induced cDNA encoding deoxyhypusine synthase and eukaryotic translation initiation factor 5A from tomato. *J. Biol. Chem.* **276**, 17541–17549
6. Park, M.H., Wolff, E.C., and Folk, J.E. (1993) Hypusine: its post-translational formation in eukaryotic initiation factor 5A and its potential role in cellular regulation. *Biofactors* **4**, 95–104
7. Chen, K.Y. and Liu, A.Y. (1997) Biochemistry and function of hypusine formation on eukaryotic initiation factor 5A. *Biol. Signals* **6**, 105–109
8. Park, M.H., Cooper, H.I., and Folk, J.E. (1982) The biosynthesis of protein-bound hypusine (N-epsilon-(4-amino-2-hydroxybutyl) lysine). Lysine as the amino acid precursor and the intermediate role of deoxyhypusine (N-epsilon-(4-aminobutyl) lysine). *J. Biol. Chem.* **257**, 7219–7222
9. Park, M.H. and Wolff, E.C. (1988) Cell-free synthesis of deoxyhypusine. Separation of protein substrate and enzyme and identification of 1,3-diaminopropane as a product of spermidine cleavage. *J. Biol. Chem.* **263**, 15264–15269
10. Wolff, E.C., Park, M.H., and Folk, J.E. (1990) Cleavage of spermidine as the first step in deoxyhypusine synthesis. The role of NAD. *J. Biol. Chem.* **265**, 4793–4799
11. Park, M.H., Lee, Y.B., and Joe, Y.A. (1997) Hypusine is essential for eukaryotic cell proliferation. *Biol. Signals* **6**, 115–123
12. Park, M.H., Joe, Y.A., and Kang, K.R. (1998) Deoxyhypusine synthase activity is essential for cell viability in the yeast *Saccharomyces cerevisiae*. *J. Biol. Chem.* **273**, 1677–1683
13. Schnier, J., Schwelberger, H.G., Smit-McBride, Z., Kang, H.A., and Hershey, J.W.B. (1991) Translation initiation factor 5A and its hypusine modification are essential for cell viability in the yeast *Saccharomyces cerevisiae*. *Mol. Cell. Biol.* **11**, 3105–3144
14. Sasaki, K., Abid, M.R., and Miyazaki, M. (1996) Deoxyhypusine synthase gene is essential for cell viability in the yeast *Saccharomyces cerevisiae*. *FEBS Lett.* **384**, 151–154
15. Xu, A. and Chen, K.Y. (2001) Hypusine is required for a sequence-specific interaction of eukaryotic initiation factor 5A with postsystematic evolution of ligands by exponential enrichment RNA. *J. Biol. Chem.* **276**, 2555–2561
16. Kawarabayashi, Y., Sawada, M., Horikawa, H., Haikawa, Y., Hino, Y., Yamamoto, S., Sekine, M., Baba, S., Kosugi, H., Hosoyama, A., Nagai, Y., Sakai, M., Ogura, K., Otsuka, R., Nakazawa, H., Takamiya, M., Ohfuku, Y., Funahashi, T., Tanaka, T., Kudoh, Y., Yamazaki, J., Kushida, N., Oguchi, A., Aoki, K., and Kikuchi, H. (1998) Complete sequence and gene organization of the genome of a hyper-thermophilic archaebacterium, *Pyrococcus horikoshii* OT3. *DNA Res.* **5**, 55–76
17. Kim, K.K., Hung, L-W., Yokota, H., Kim, R., and Kim, S-H. (1998) Crystal structure of eukaryotic translation initiation factor 5A from *Methanococcus jannaschii* at 1.8 Å resolution. *Proc. Natl. Acad. Sci. USA* **95**, 10419–10424
18. Peat, T.S., Newman, J., Waldo, G.S., Berendzen, J., and Terwilliger, T.C. (1998) Structure of translation initiation factor

5A from *Pyrobaculum aerophilum* at 1.75 Å resolution. *Structure* **6**, 1207–1214
19. Studier, F.W., Rosenberg, A.H., Dunn, J.J., and Dubendorff, J.W. (1990) Use of T7 RNA polymerase to direct the expression of cloned genes. *Methods Enzymol.* **185**, 60–89
20. Leslie, A.G.W. (1993) Auto-indexing of rotation diffraction images and parameter refinement in *Proceeding of the CCP4 Study Weekend* (Sawyer, L., Isaacs, N., and Bailey, S., eds.) pp. 44–51, Daresbury Laboratory, Daresbury, UK
21. Evans, P.R. (1997) Scaling of MAD data in *Proceeding of the CCP4 Study Weekend* (Wilson, K.S., Davies, G., Ashton, A.W., and Bailey, S., eds.) pp. 97–102, Daresbury Laboratory, Daresbury, UK
22. Mattews, B.W. (1968) Solvent content of protein crystal. *J. Mol. Biol.* **33**, 491–497
23. Vagin, A. and Teplyakov, A. (1997) MOLREP: An automated program for molecular replacement. *J. Appl. Crystallogr.* **30**, 1022–1025
24. Brunger, A.T., Adams, P.D., Clore, G.M., Delano, W.L., Gros, P., Grosse-Kunstleve, R.W., Jlang, J-S., Kuszewski, J., Nilges, N., Pannu, N.S., Read, R.J., Rice, L.M., Simonson, T., and Warren, G.L. (1998) Crystallography and NMR System (CNS): A new software system for macromolecular structure determination. *Acta Crystallogr. D* **54**, 905–921
25. Jones, T.A., Zou, J.Y., Cowan, S.W., and Kjeldgaard, M. (1991) Improved methods for building protein models in electron density maps and the location of errors in these models. *Acta Crystallogr. A* **47**, 110–119
26. Laskowski, R.A., MacArthur, M.W., Moss, D.S., and Thornton, J.M. (1993) PROCHECK: a program to check the stereochemical quality of protein structures. *J. Appl. Crystallogr.* **26**, 283–291
27. Kabsch, W. and Sander, C. (1983) Dictionary of protein secondary structures: Pattern recognition of hydrogen-bonded and geometrical features. *Biopolymers* **22**, 2577–2637
28. Thompson, J.D., Higgins, D.G., and Gibson, T.J. (1994) CLUSTAL W: improving the sensitivity of progressive multiple sequence alignment through sequence weighting, position-specific gap penalties and weight matrix choice. *Nucleic Acids Res.* **22**, 4673–4680
29. Kabsch, W. (1976) A solution for the best rotation to relate two sets of vectors. *Acta Cryst. A* **32**, 922–923
30. Holm, L. and Sander, C. (1993) Protein structure comparison by alignment of distance matrices. *J. Mol. Biol.* **233**, 123–138
31. Lodi, P.J., Ernst, J.A., Kuszewski, J., Hickman, A.B., Engelman, A., Craigie, R., Clore, G.M., and Gronenborn, A.M. (1995) Solution structure of the DNA binding domain of HIV-1 integrase. *Biochemistry* **34**, 9826–9833
32. Wilson, K.P., Shewchuk, L.M., Brennan, R.G., Otsuka, A.J., and Mathews, B.W. (1992) *Escherichia coli* biotin hole enzyme synthetase/bio repressor crystal structure delineates the biotin- and DNA-binding domains. *Proc. Natl. Acad. Sci. USA* **89**, 9257–9261
33. Nakagawa, A., Nakashima, T., Taniguchi, M., Hosaka, H., Kimura, M., and Tanaka, I. (1999) The three-dimensional structure of the RNA-binding domain of ribosomal protein L2; a protein at the peptidyl transferase center of the ribosome. *EMBO J.* **18**, 1459–1467
34. Sette, M., van Tilborg, P., Spurio, R., Kaptein, R., Paci, M., Gualerzi, C.O., and Boelens, R. (1997) The structure of the translational initiation factor IF1 from *E. coli* contains an oligomer-binding motif. *EMBO J.* **16**, 1436–1443
35. Nonato, M.C., Widom, J., and Clardy, J. (2002) Crystal structure of the N-terminal segment of human eukaryotic translation initiation factor 2α. *J. Biol. Chem.* **277**, 17057–17061
36. Bycroft, M., Hubbard, T.J., Proctor, M., Freund, S.M., and Murzin, A.G. (1997) The solution structure of the S1 RNA binding domain: a member of an ancient nucleic acid-binding fold. *Cell* **88**, 235–242
37. Golden, B.L., Hoffman, D.W., Ramakrishnan, V., and White, S.W. (1993) Ribosomal protein S17: characterization of the three-dimensional structure by ^{1}H and ^{15}N NMR. *Biochemistry* **32**, 12812–12820
38. Ruff, M., Krishnaswamy, S., Boeglin, M., Poterszman, A., Mitschler, A., Podjarny, A., Rees, B., Thierry, J.C., and Moras, D. (1991) Class II aminoacyl transfer RNA synthetases: crystal structure of yeast aspartyl-tRNA synthetase complexed with tRNA(Asp). *Science* **252**, 1682–1689
39. Liu, Y.P., Nemeroff, M., Yan, Y.P., and Chen, K.Y. (1997) Interaction of eukaryotic initiation factor 5A with the human immunodeficiency virus type 1 Rev response element RNA and U6 snRNA requires deoxyhypusine or hypusine modification. *Biol. Signals* **6**, 166–174
40. Burd, C.G. and Dreyfuss, G. (1994) Conserved structures and diversity of functions of RNA-binding proteins. *Science* **265**, 615–621
41. Lee, Y.B., Joe, Y.A., Wolff, E.C., Dimitriadis, E.K., and Park, M.H. (1999) Complex formation between deoxyhypusine synthase and its protein substrate, the eukaryotic translation initiation factor 5A (eIF5A) precursor. *Biochem. J.* **340**, 273–281
42. Singh, U.S., Li, Q., and Cerione, R. (1998) Identification of the eukaryotic initiation factor 5A as a retinoic acid-stimulated cellular binding partner for tissue transglutaminase II. *J. Biol. Chem.* **273**, 1946–1950
43. Schatz, O., Oft, M., Dascher, C., Schebesta, M., Rosorius, O., Jaksche, H., Dobrovnik, M., Bevec, D., and Hauber, J. (1998) Interaction of the HIV-1 Rev cofactor eukaryotic initiation factor 5A with ribosomal protein L5. *Proc. Natl. Acad. Sci. USA* **95**, 1607–1612
44. Elfgang, C., Rosorius, O., Hofer, L., Jaksche, H., Hauber, J., and Bevec, D. (1999) Evidence for specific nucleocytoplasmic transport pathways used by leucine-rich nuclear export signals. *Proc. Natl. Acad. Sci. USA* **96**, 6229–6234
45. Lipowsky, G., Bischoff, F.R., Schwarzmaier, P., Kraft, R., Kostka, S., Hartmann, E., Kutay, U., and Gorlich, D. (2000) Exportin 4: a mediator of a novel nuclear export pathway in higher eukaryotes. *EMBO J.* **19**, 4362–4371
46. Nicholls, A., Sharp, K., and Honig, B. (1991) Protein folding and association; insights from the interfacial and thermodynamic properties of hydrocarbons. *Proteins Struct. Funct. Genet.* **11**, 281–296